Classification of Floodplain Habitats (Lago Grande, Brazilian Amazon) with RADARSAT and JERS-1 Data.

(*) Maycira P. F. Costa; Evlyn M.L.M. Novo; Fernando Mitsuo II, José E. Mantovani;
(**) Maria Victoria Ballester; (***) Frank Ahern.

(*) Instituto Nacional de Pesquisas Especiais
Divisão de Sensoriamento Remoto
Avenida dos Astronautas, 1758
12227-010 São José dos Campos, SP, Brasil.

(**) Centro de Energia Nuclear para a Agricultura, CENA, Piracicaba, SP, Brasil.

(***) Canada Center for Remote Sensing.
588 Booth St., Ottawa, Ontario, K1A 0Y7.

Abstract

Constant cloud cover and dense forest canopy prevent the application of optical remote sensing for the classification of floodplain habitats in the Amazon region. Although several attempts have been made for using Thematic Mapper, the reported results are still incomplete.

Multitemporal (May and August, 1996) RADARSAT and JERS-1 radar images were used to investigate the potential of using multi-incidence angle and multiwavelength radar data for increasing digital classification accuracy. Floodplain habitats that are of interest for a preliminary classification are open water, flooded forest, non-flooded forest, aquatic plants and landuse/landcover. Subset of the Lago Grande scene were selected for a preliminary assessment of the methodology and the classification accuracy.

Raw radar data had to be converted into a near-normal distribution by applying a filtering procedure on each data set. RADARSAT, JERS-1 and a combination of both images were submitted to a segmentation process using different thresholds according to pixel number and similarity. After this procedure, each segmented image had a Bhattacharya distance classification algorithm applied. The results were then verified with aerial photographs and ground truth information that had been collected concurrently with the radar image acquisition.

1. Introduction

A precise measure of the area occupied by the Amazon floodplain does not exist yet. Some authors have shown estimates based on various sources such as extrapolated data or optical (Landsat) and radar (RADAMBRASIL) images (Melack and Fisher, 1989; Sippel et al., 1992). The problem with those sources are the lack of information on seasonal changes in the flooded area, the poor scale in the case of RADAMBRASIL and the out-dated data.

The knowledge of the area accupied by the Amazon floodplain and its distinct habitats is important not only in a local scale, but also in a global scale. The hydrological cycle dynamic in the floodplain provides a unique condition to create the complex ecosystem of the Amazon floodplain. The lakes are important spawn areas for some fishes species. The annual flooded forest is an important source of food for the fruit- and seed-eating fishes, such as *Colossoma Macropomum* (tambaqui). It is also a refuge area for fishes. The large areas populated by aquatic plants are important areas for feeding and protection of young fishes. Also, the aquatic

plants are considered one of the most important sources of nutrients to the Amazon waters (Goulding and Smith, 1997).

The Amazon floodplain also plays an important role to understand the global carbon cycle as a source/or sink of atmospheric methane (Climate Change, 1995). For example, the floodplain inundated by white water rivers are a natural source of methane and others gases contributing to the greenhouse effects (Junk et al., 1993). The methane fluxes of the Amazon Basin (floodplain areas, floating aquatic plants, flooded forest and open water) appear to be relatively high when compared with other wetland emissions rates (Bartellet and Harris, 1993). The total amount of methane emission is highly dependent on the extent of the inundated area, and on the fraction of the different habitats in the floodplain.

One of the first attempts of mapping the Amazon floodplain was the RADAMBRASIL project (Radambrasil, 1976). The results are very important but not provide information at good scale and seasonally. Other results were achieved using Landsat data, which is subjected to intense cloud cover precluding the seasonal information as well. This data, however, has already been used to estimate the proportion of the different habitats within the Amazon floodplain (Mertes, 1995; Shimabukuro et al., 1997). SAR data provided by satellites, such as ERS 1/2, JERS 1 and RADARSAT are important source of information for tropical areas due to its all weather acquisition functionality.

Due to the huge dimension and the seasonal variation of the Amazon floodplain and its distinct habitats, a visual interpretation of satellite data would not be an efficient method for mapping the floodplain. Some authors (Hess et al., 1995) have already shown very good results of digital classification of the Amazon floodplain using fine resolution, multipolarization and multifrequency SAR data acquired during the SIR-C/X mission.

The conventional classification of images acquired by optical sensors is based on statistics. This method is a punctual analyses and is based on the spectral attributes of the pixels, which depends on the spectral characteristics of the target, sensor calibration, illumination, geometry and atmosphere conditions. Radar data, alternatively, would not depend on the illumination and atmosphere conditions. The radar sensor response depends basically on the interaction of the target with the microwave radiation, the sensor calibration and the geometry of acquisition. The undesirable effect in the images is the speckel noise, which can be a problem for a per-pixel classification method. The speckel effect is caused by the coherent interference of the backscattered radiation from the scattering elements of the terrain (Ulaby et al., 1986). There have been several attempts to use multipolarization, multiwavelength SAR data to classify land-cover. Some authors show interesting results with knowledge-based classification, based on physical principles (Pierce et al., 1994; Dobson et al., 1996). Other authors have shown adequate results for crop digital classification based on maximum likelihood and textural measures (Anys and He, 1995).

An alternative approach for SAR images classification is an image pre-segmentation. Segmentation procedure based on the successive application of a speckle filter was successfully applied to ERS-1 images of sea ice (Smith, 1996). According to the author further work is required to evaluate other segmentation methods, including those based on edge-detection and region growing. Lobo et al., (1996) also reported that segmentation of SAR and TM/Landsat images, and classification through linear canonical discriminant analysis is a good approach for classifying crop fields.

In this study we processed a multisensor (JERS-1 and RADARSAT) image date set of a test site in the Amazon floodplain to evaluate floodplain habitats discrimination based on digital segmentation and classification.

2. Study Site and SAR Data.

The study area is Monte Alegre lake (2°10'S/54° 20'W) in the northeast of the Brazilian Amazon (Fig. 1). The Lake has approximately 70 Km of length, depending on the flooded stage of the Amazon and Tapajós rivers. The lake is connected to the Amazon river through narrow channels and to the Maicurú river. The high water level in the lake is reported with the maximum water level of Tapajós, Maicurú and Amazon rivers (April and May), promoting an yearly water level variation around 5 to 7 meters.

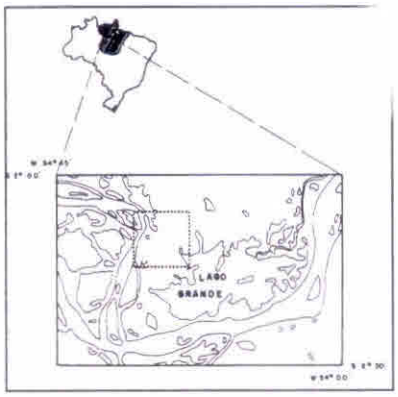

Fig. 1. Study site.

An area of approximately 20x20 km (Fig. 1) was selected as a test site to perform the classification procedure. This area was selected due to the availability of aerial photographs and data of field work, which allow us to evaluate the performance of the classifier.

The test site is geomorphologically characterized by a seasonally flooded area (Maicurú river region) and higher land area with intensive anthropic use as pasture and small agriculture fields. The seasonally flooded area includes a wide variety of aquatic plants and inundated trees. Among the aquatic vegetation we can exemplify *Paspalun repens* (premembeca), *Orzya* spp. (arroz selvagem), *Montrichardia arborescens* (aninga) as shown by Costa et al., 1997. The average high of the aquatic plants in the area is one meter and the wet biomass 4591 gm^{-2} (Novo et al., 1997). The inundated forest is colonized by several different species of trees such as *Astrycaryum jauari* (jauarí) and *Pseudobombax munguba* (munguba) The last one loses the leaves in the high water season (May).

The data set for the study consisted of aerial photography, RADARSAT and JERS-1 images and field observations such as hand-help photographs, collect GPS coordinates and field description of the test site. The color aerial photographs were acquired at 1:20 000 scale at the end of May, 1996. They were scanned, mosaicked, visually interpreted and subsequently digitized for creating a digital land cover map. The resultant map was used as a ground truth map.

Table 1 summarizes the date acquisition of the satellite data. A better description of the data set can be find in Costa et al., 1997. The water level data was obtained from the Brazilian navy gauge in the Tapajós river near to Santarém. The higher and lower water levels are reported as being on May and November, respectively.

Tabela 1. Data set acquisition date.

Image	lgJM	lgS6M	lgS1M	lgJJ	lgS6A
sensor	Jers-1	Radarsat	Radarsat	Jers-1	Radarsat
Date	16.05.96	27.05.96	30.05.96	29.06.96	07.08.96
water level (meters)	8.05	7.8	7.8	7.6	6.9

3. Satellite data processing.

The Figure 2 shows a flowchart of the digital processing steps. The images were ortho-rectified according to the methodology developed by Toutin, (1995). The accuracy of the model was on average 11.4 meters and the accuracy of the restitution was on average 19.2 meters, and the final resolution was 12.5 meters. Detailed information about the images ortho-correction are reported by Costa et al., 1997.

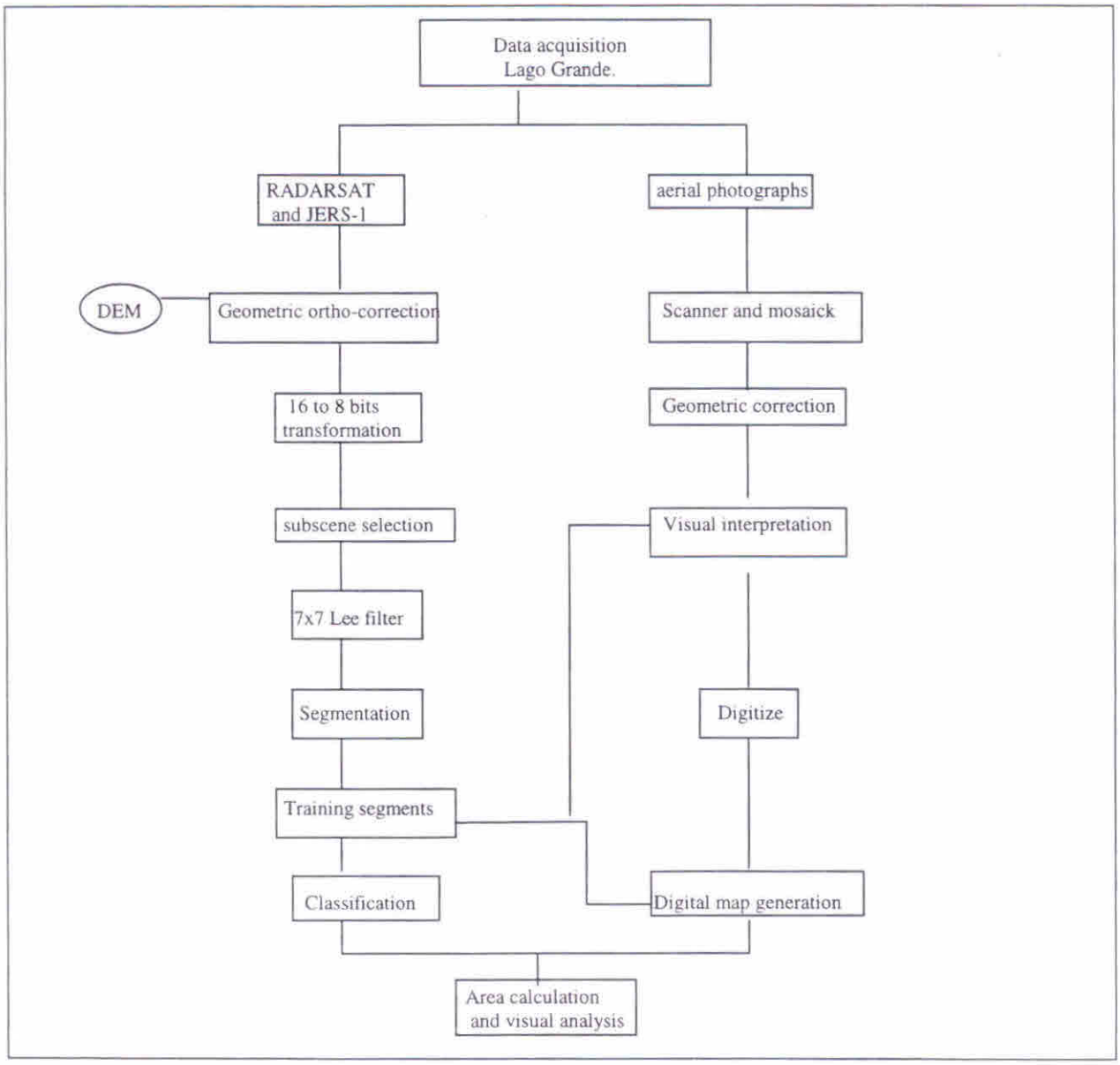

Fig. 2. Digital processing steps.

The segmentation and classification processes could only be carried out within an 8-bit dynamic range data. So that, a linear scaling transformation from 16 to 8 bit was performed. The linear scaling was performed trying to optimize the useful dynamic range of each data, which provides a better contrast within the scene.

A subscene of approximately 20 x 20 Km near to the Maicurú river was selected. The area was selected due to the availability of aerial photographs and also the presence of the five classes of interest: water, aquatic plants, flooded forest, forest and pasture. This classes are useful not only for methane emission estimation, but also for future monitoring of the deforestation of forest, flooded forest and aquatic vegetation.

The speckle noise degrades both the radiometric and textural information of SAR images, being a undesirable effect for digital classification. One way to reduce speckle while preserves the texture is the use of adaptive filters (Lopes at al., 1990). Different filters were tested with the data set such as: median, average, Frost, Fgamma and Lee. The best result was obtained with Lee filter. Therefore, unspeckled Radarsat and Jers-1 images were obtained by applying Lee filter (7x7 window), which reduces the additive and multiplicative noise.

In order to perform the classification process the images were segmented. Image segmentation is often based on edge detection and region growing. The region growing technique is an interactive process by which regions are merged starting from individual pixels, and growing interactively until every pixel is processed. The user must manually provides the similarity and an area thresholds which depend on the data type and the user needs (Bins, et al. 1996). Radarsat and Jers-1 and a combination of both images were submitted to a segmentation process using different thresholds according to pixel number and digital number similarity. Different thresholds combination were tested, either for single data or for a combination of both, Radarsat and Jers-1. Figure 3 shows a segmentation of a Radarsat S6 and a Jers-1, both acquired in May and Figure 4 shows the radar color composition. Table 2 shows how the data set was organized for performing the segmentation and the selected thresholds.

Table 2. Segmented data set.

	lgJM	lgRS6M	lgRS6MJM	lgJJ	lgRS6A	lgRS6AJJ	lgRS1M	lgRS1MJM
Data	Jers-1, May	Radarsat S6, May	RadarsatS6 +Jers1,May	Jers1, June	Radarsat S6,August	RadarsatS6 (August)+ Jers1(June)	Radarsat S1, May	RadarsatS1 +Jers1,May
Area threshold	50	50	50	50	50	50	50	50
Similarity threshold	20	20	30	20	20	30	20	30

A supervised classification was performed in each pre-segmented image according to the Bhattacharrya distance algorithm (Richards, 1986). The training segments were selected according to the ground truth map, generated from the aerial photograph mosaic.

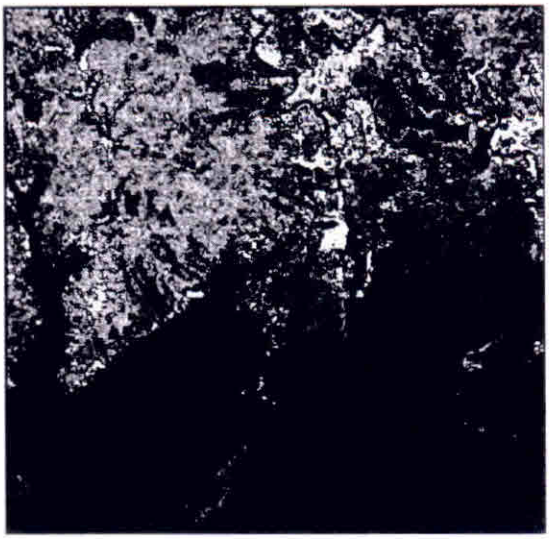

Figure 3. Segmentation of Radarsat S6 and Jers-1, May.

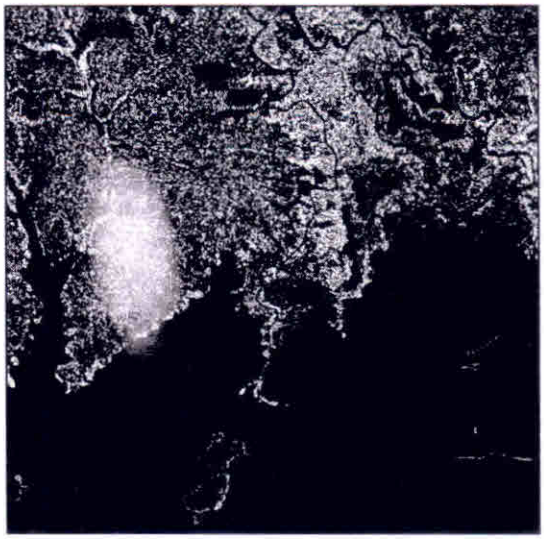

Figure 4. Color composite, Radarsat S6,May (red); Jers-1,May (green); and Jers-1 August (blue).

4. Results and Discussion

The following discussion is based on both the visual inspection of the SAR classification results and on the quantitative area results generated from the classified images. Table 3 summarizes the calculated area for each classified class. The ground truth map data has an extra class (no-data), which represents lack of information in the area. To overcame this lack of information the ground truth map was compared with the images and the "no-data" class was associated to the other classes. Therefore, it must be considered that the no-data area generated from the ground truth map corresponds, at least, to approximately 80 km^2 of water, 20 km^2 of forest and the remaining area (18.4 km^2) could be part of flooded-forest, pasture and aquatic-plants classes. The parenthesis values in Table 3 correspond to the area values for the ground truth map data supposing this approach.

Table 3. Calculated area for the classified data.

	Water	Forest	Flooded-forest	Aquatic-plants	Pasture	no data
ground truth map	82.4 (162.4)	43.6 (63.6)	33.0 (?)	41.3 (?)	28.5 (?)	118.4
JM	167.9	72.9	24.6	43.1	42.55	
RS6M	164.4	77.8	21.1	64.2	23.5	
RS6MJM	159.9	78.72	31.1	57.35	23.9	
JJ	166.9	71.5	31.5	44.0	37.1	
RS6A	169.1	71.1	16.9	61.3	32.9	
RS6AJJ	168.46	70.0	27.5	53.3	31.7	
RS1M	164.86	85.2	36.9	43.2	20.8	
RS1MJM	165.8	72.1	29.8	56.6	26.7	

It was observed an improved classification when Jers-1 and Radarsat are used in combination (Figs. 5b, 6a and 7a) when compared with the digital ground truth map (Fig. 5a). The reasons for that are the distinct incidence angle, wavelength and date. Some differences were observed between the result of the classification of Radarsat and Jers-1, also dependent on the acquisition date.

The results yield a similar water class area independent of the data set used to run the digital classification. However, the visual inspection of the digital classified maps shows that RADARSAT provides a better discrimination of the narrow water channels. Jers-1 misclassification, for water class, is probably caused by the low backscattering of the radar signal by the water, aquatic-plants (blade-like leaves) and pasture classes. Short blade-like vegetation would represent low roughness at L-band, and consequently low backscattering.

The forest region is not a typical Amazon dense rainforest. It is characterized by not so dense trees (savanna) and for soil covered with griminea or even baresoil. This could be one of the reasons for the misclassification of forest (or savanna) and pasture classes, mainly in C-band. The misclassification is obvious in the visual inspection of the digital classified maps, and in the higher area values obtained from the classified data. In August, the Radarsat S6 mode (Fig. 6b) shows a better separability between pasture and forest, when compared with Radarsat image from May. This result can be explained by the drier condition in August.

The Figures 8a and 8b show the average digital numbers (DN) average values of the training segments. It can be observed that the DN values of the pasture class is about the same for both sensors and also that the forest DN values are in the same range in the case of Radarsat. Therefore, the combination of both sensors provides a better classification of forest and pasture. Due to the low backscattering of Jers-1 for aquatic plants and pasture areas, some misinterpretation is observed in individual Jers-1 images classification. A misclassification between aquatic plants and flooded forest is observed for Radarsat S6 images. The main reason would be the lower penetration of C-band in the flooded forest canopy, resulting in a not so powerful double-bounce effect, and consequently showing almost the same backscattering values of the grass-like aquatic-plants (1 meter high). Previous papers indicated that standing water beneath a canopy strongly reinforces backscatter at L-band with HH polarization (Richards et al., 1987; Ford and Casey, 1988). The same result is observed with Jers-1 data, showing a very good discrimination between flooded-forest and aquatic-plants (Fig. 5d and 6c). It is interesting to notice that Radarsat S1 mode (lgS1M) shows a better separability between aquatic plants and flooded forest (Fig. 7b), when compared with S6 mode. This result can be explained by the steeper incidence angle of S1 mode (20°-27°), which means an additional penetration of the microwave energy into the flooded forest canopy producing a double-bounce effect (Hess et al., 1990).

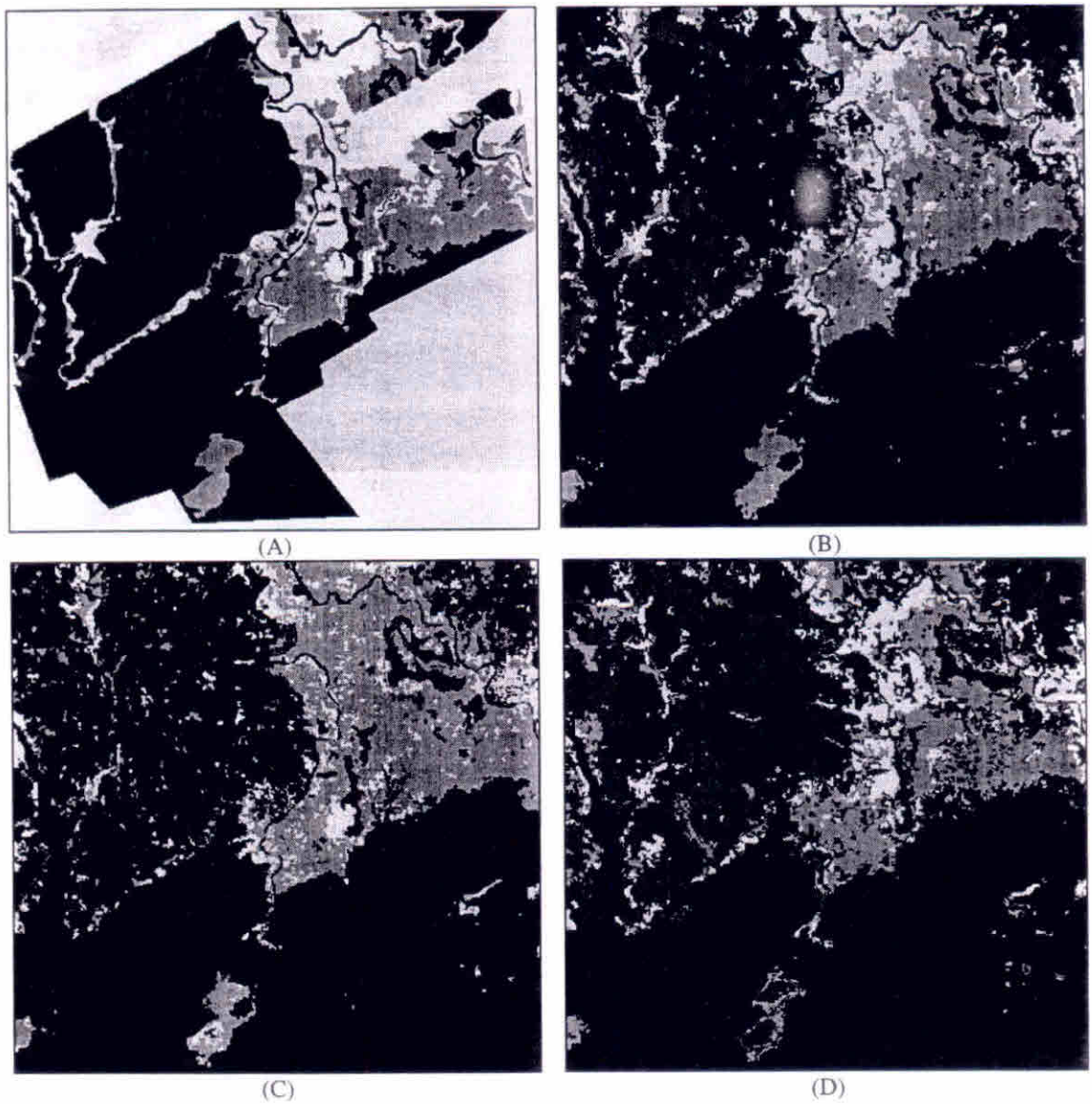

Fig. 5. (A) - Digital ground truth map. (B)-Classification of Radarsat S6 and Jers-1, May. (C)- Classification of Radarsat S6, May. (D)- Classification of Jers-1, May. GREEN=forest; BLUE=water; ORANGE=pasture; YELLOW=flooded forest; CYAN=aquatic plants.

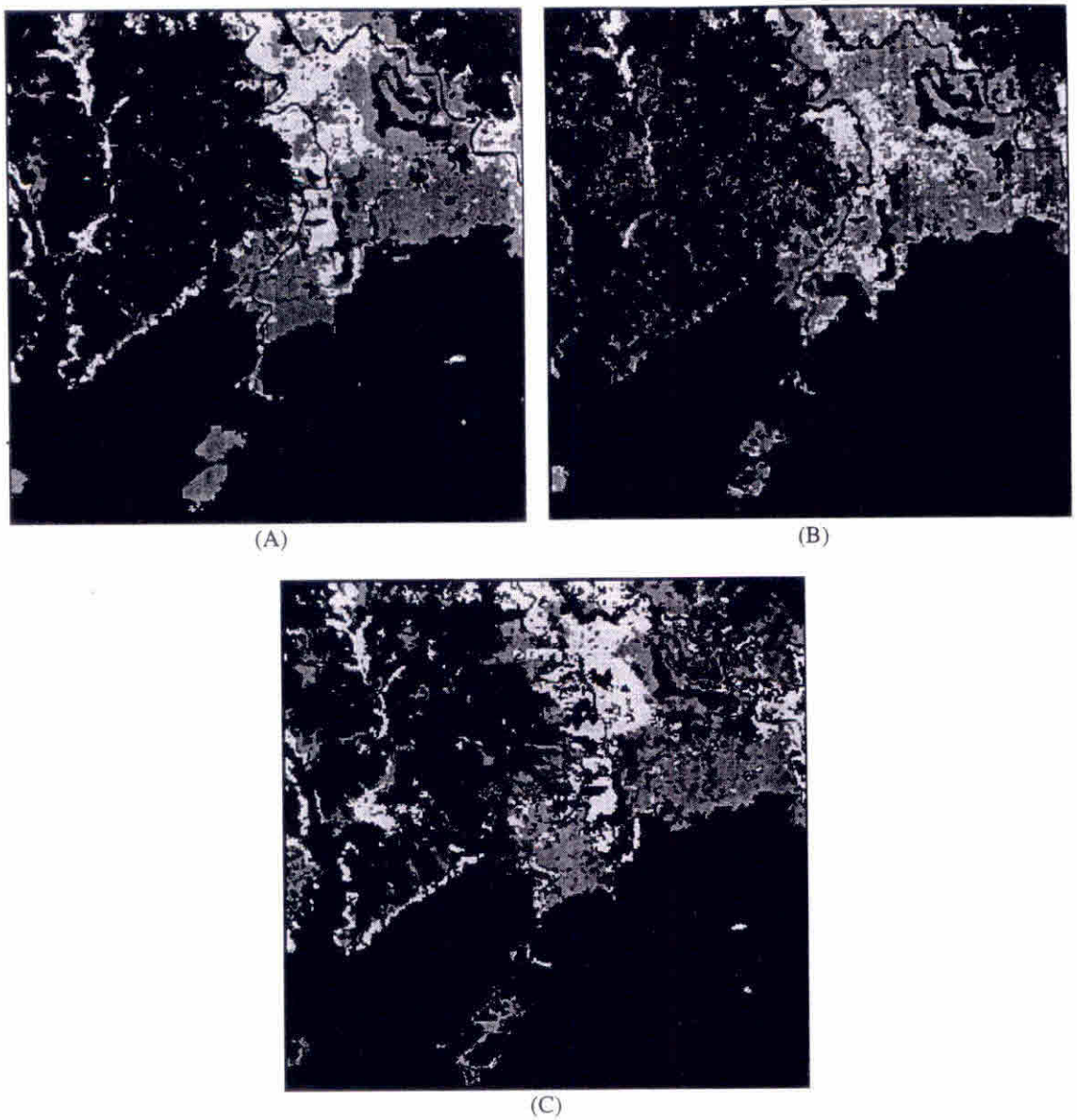

Figure 6. (A)-Classification of Radarsat S6 (August) and Jers-1 (June). (B)- Classification of Radarsat S6, August. (C)- Classification of Jers-1, June. GREEN=forest; BLUE=water; ORANGE=pasture; YELLOW=flooded forest; CYAN=aquatic plants.

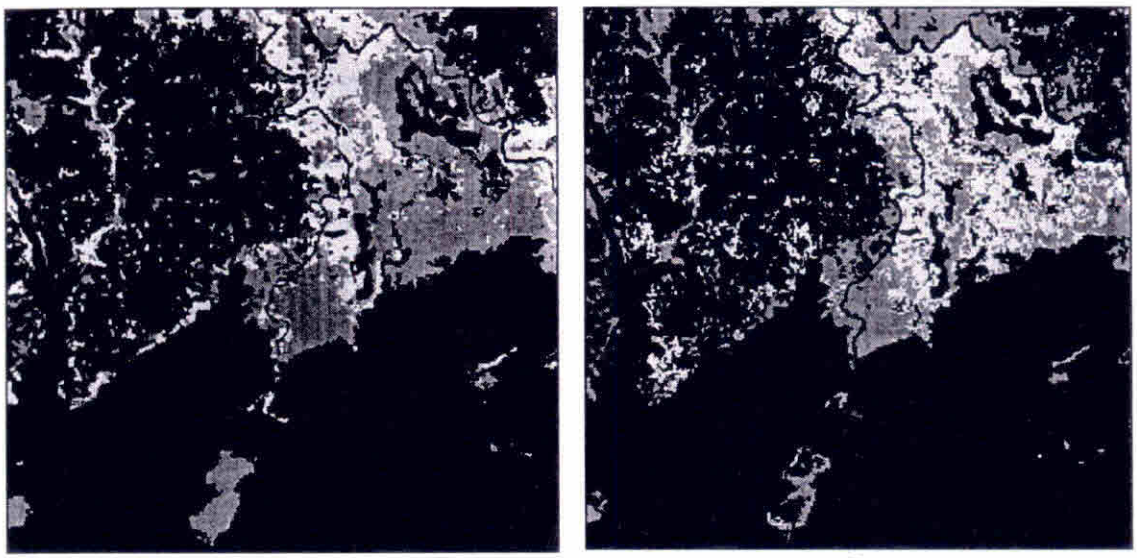

(A) (B)

Figure 7. (A)-Classification of Radarsat S1 and Jers-1, May. (B)- Classification of Radarsat S1, May. (C)- Classification of Jers-1, May. GREEN=forest; BLUE=water; ORANGE=pasture; YELLOW=flooded forest; CYAN=aquatic plants.

5. Conclusion

A segmentation and classification process has been performed in Radarsat and Jers-1 multitemporal images. Radarsat S6 image alone performs poorly for classifying pasture and forest areas, with a better result for image acquired in the dry season. Radarsat S1 image provides a better separability between aquatic plants and flooded forest area when compared with S6 images. Also, Radarsat provides a better classification of narrow water channels than Jers-1.

When using Jers-1 alone, the overall classification is better than Radarsat alone, for the classified classes. However, there is still misinterpretation of pasture and aquatic plants areas. In all cases, the results show that either in terms of calculated areas or in terms of visual inspection of the classified images the applied classification methodology does significantly better for the two sensors composite than for the individual images classification. This is an important result for verifying the complementarity of multiwavelangth, multi-incidence angle and multitemporal SAR data.

Although the results presented here are just for a subscene of the distinct images, the segmentation and Battacharya classification showed a valuable potential for SAR images classification. The next step will be apply the same methodology for the whole images and also test a knowledge-base classifier, as already suggested by Dobson et al., 1996.

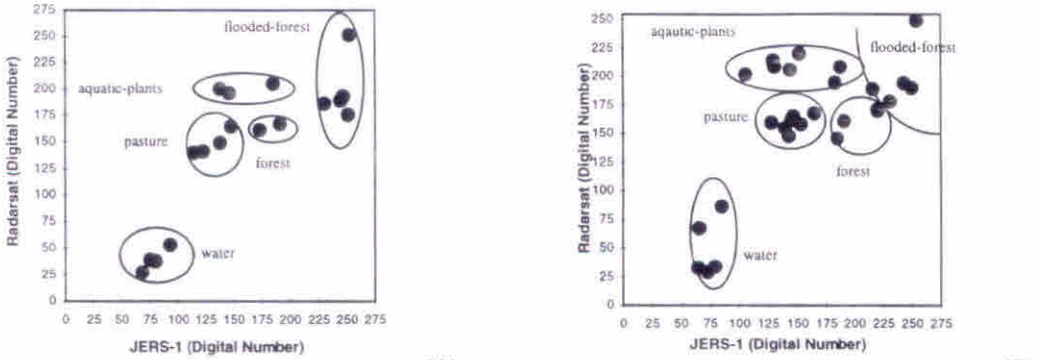

Fig. 8. (A) - Radarsat S6 August 1996 and Jers-1, June, 1996. (B) - Radarsat S1, May 1996 and Jers-1, May 1996.

References

ANYS, H.; HE, D. C., 1995. Evaluation of textural and mutlipolarization radar features for crop classification. *IEEE Transaction on Geoscience and Remote Sensing*, 33(5):1170-1181.

BARTLETT, K.B.; HARRIS, R.C., 1993. Review and assessment of methane emissions from wetlands. *Chemosphere*,26(1-4):261-320.

COSTA, M.P.F.; NOVO, E.M.L.M.; PIETSCH, R.W.; AHERN, F., 1997. Pre-processing of RADARSAT images of Tucuruí reservoir and Lago Grande floodplain, Amazon. *GER'97*, May 25-30, Ottawa, Canada.

BINS, L.S.; FONSECA, L.M.G., ERTHAL, G.J. MITSUO, F., 1996. Stellite imagery segmentation: a region growing approach. In: Simpósio Brasileiro de Sensoriamento Remoto. Salvador, Bahia, Brasil.

DOBSON M.C.; PIERCE,L.E.; ULABY, F.T., 1996. Knowledge-based land-cover classification using ERS-1/JERS-1 SAR composites. *IEEE Transaction on Geoscience and Remote Sensing*. 34(1):83-99.

FORD, J.P.; CASEY, D.J., 1988. Shuttle radar mapping with diverse incidence angles in the rainforest of Borneo. *International Journal of Remote Sensing*. 9(5):927-943.

GOULDING, M.; SMITH, N.J.H., 1996. *Floods of Fortune - Ecology & Economy Along the Amazon*. Columbia University Press, New York. 193p.

HESS, L.L.; MELACK,J.M.; FILOSO, S.; WANG, Y., 1995. Delineation of inundated area and vegetation along the Amazon Floodplain with SIR-C synthetic aperture radar. *IEEE Transaction on Geoscience and Remote Sensing*. 33(4):896-903.

HESS, L.; MELACK,J.M.; SIMONETT, D., 1990. Radar detection of flooding beneath the forest canopy: a review. *International Journal of Remote Sensing*. 11(7):1313-1325.

LOBO, A.; CHIC, O.; CASTERAD, A., 1996. Classification of Mediterranean crops with multisensor data: per-pixel versus per-object statistics and image segmentation. *International Journal of Remote Sensing*. 17(12):2385-2400.

MERTES, L.A.K.; DANIEL, D.L.; MELACK, J.M.; NELSON, B. MARTINELLI, L.A.; FORSBERG, B.R., 1995. Spatial patterns of hydrology, geomorphology, and vegetation on the floodplain of the Amazon in Brazil from a remoite sensing perspective. *Gemomorphology*. 13:215-232.

NOVO, E.M.L.N.; COSTA, M.P.F.; MANTOVANI, J.E., BALLESTER,M.V., 1997. RADARSAT relative backscatter and macrophyte canopy variables: preliminary results for Tucuruí reservoir and lago Grande floodplain, Brazilian Amazon. GER'97, May 25-30, Ottawa, Canada.

PIERCE, L.E.; ULABY, F.T.; SARABANDI, K.; DOBSON, M.C., 1994. Knowledge-based classification of polarimetric SAR images. *IEEE Transaction on Geoscience and Remote Sensing*. 32(5):1081-1086.

RICHARDS, J.A., 1986. *Remote Sensing Digital Image Analysis*. Spring-Verlag (ed.) 281 p.

RICHARDS, J.A.; WOODGATE, P.W.; SKIDMORE, A.K., 1987. An explanation of enhenced radar backscattering from flooded forest. *International Journal of Remote Sensing*. 8(7):1093-1100.

SIPPEL, S.J.; HAMILTON, S.K.; MELACK, J.M., 1992. Inundation area and morphometry of lakes on the Amazon rever floodplain, Brazil. *Arch. Hydrobiology*. 123(4):385-400.

SMITH, D.M., 1996. Speckle reduction and segementation of synthetic aperture radar images. *International Journal of Remote Sensing*. 17(11):2043-2057.

TOUTIN, T., 1995. Multisource data integration with an integrated and unified geometric modelling. In: Sensors and Environment Applications of Remote Sensing. *Proceedings*. Askne (ed.), Balkema, Rotterdan. pp:163-469.

ULABY, F.T.; MOORE,R.K.; FUNK, A.K., 1986. *Microwave Remote Sensing*.